

# Accepted Manuscript

New insight into the structural, electrochemical and biological aspects of macrocyclic Cu(II) complexes derived from S-substituted dithiocarbazate schiff bases

May Lee Low, Laure Maigre, Mohamed Ibrahim M. Tahir, Edward R.T. Tiekink, Pierre Dorlet, Régis Guillot, Thahira Begum Ravoof, Rozita Rosli, Jean-Marie Pagès, Clotilde Policar, Nicolas Delsuc, Karen A. Crouse

PII: S0223-5234(16)30320-8

DOI: [10.1016/j.ejmech.2016.04.027](https://doi.org/10.1016/j.ejmech.2016.04.027)

Reference: EJMECH 8542

To appear in: *European Journal of Medicinal Chemistry*

Received Date: 31 August 2015

Revised Date: 25 March 2016

Accepted Date: 9 April 2016

Please cite this article as: M. Lee Low, L. Maigre, M.I.M. Tahir, E.R.T. Tiekink, P. Dorlet, R. Guillot, T.B. Ravoof, R. Rosli, J.-M. Pagès, C. Policar, N. Delsuc, K.A. Crouse, New insight into the structural, electrochemical and biological aspects of macrocyclic Cu(II) complexes derived from S-substituted dithiocarbazate schiff bases, *European Journal of Medicinal Chemistry* (2016), doi: 10.1016/j.ejmech.2016.04.027.

This is a PDF file of an unedited manuscript that has been accepted for publication. As a service to our customers we are providing this early version of the manuscript. The manuscript will undergo copyediting, typesetting, and review of the resulting proof before it is published in its final form. Please note that during the production process errors may be discovered which could affect the content, and all legal disclaimers that apply to the journal pertain.



1 **New Insight into the Structural, Electrochemical and Biological Aspects of Macroacyclic**  
2 **Cu(II) Complexes Derived from S-Substituted Dithiocarbazate Schiff Bases**

3  
4 May Lee Low<sup>a,b</sup>, Laure Maigre<sup>c</sup>, Mohamed Ibrahim M. Tahir<sup>a</sup>, Edward R. T. Tiekink<sup>d</sup>, Pierre  
5 Dorlet<sup>e</sup>, Régis Guillot<sup>f</sup>, Thahira Begum Ravoof<sup>a</sup>, Rozita Rosli<sup>g,h</sup>, Jean-Marie Pagès<sup>c</sup>, Clotilde  
6 Policar<sup>b,\*</sup>, Nicolas Delsuc<sup>b,\*</sup> and Karen A. Crouse<sup>ai,\*</sup>

7  
8 <sup>a</sup>*Department of Chemistry, Universiti Putra Malaysia, 43400 Serdang, Selangor (Malaysia), Fax: +6 03*  
9 *89435380; E-mail: [kacrouse@gmail.com](mailto:kacrouse@gmail.com)*

10 <sup>b</sup>*École Normale Supérieure-PSL Research University, Département de Chimie, Sorbonne Universités -*  
11 *UPMC Univ Paris 06, CNRS UMR 7203 LBM, 24, rue Lhomond, 75005 Paris, (France), Fax: +33 1 44 32*  
12 *24 02; E-mail: [clotilde.policar@ens.fr](mailto:clotilde.policar@ens.fr) ; [nicolas.delsuc@upmc.fr](mailto:nicolas.delsuc@upmc.fr)*

13 <sup>c</sup>*UMR-MD1, Aix-Marseille Université, IRBA, Faculté de Médecine, 27 boulevard Jean Moulin, 13385 Marseille*  
14 *(France)*

15 <sup>d</sup>*Research Centre for Crystalline Materials, Faculty of Science and Technology, Sunway University, No. 5 Jalan*  
16 *Universiti, 47500 Bandar Sunway, Selangor Darul Ehsan, (Malaysia), [edward.tiekink@gmail.com](mailto:edward.tiekink@gmail.com)*

17 <sup>e</sup>*Institute for Integrative Biology of the Cell (I2BC), Université Paris- Saclay, CEA, CNRS, Université Paris-*  
18 *Sud, Bât 532 CEA Saclay, 91191 Gif sur Yvette cedex (France)*

19 <sup>f</sup>*Institut de Chimie Moléculaire et des Matériaux d'Orsay, Bât. 420 Université Paris-Sud, 91405 Orsay (France)*

20 <sup>g</sup>*Department of Obstetrics and Gynaecology, Universiti Putra Malaysia, 43400 Serdang, Selangor (Malaysia)*

21 <sup>h</sup>*UPM-MAKNA Cancer Research Laboratory, Institute of Bioscience, Universiti Putra Malaysia, 43400*  
22 *Serdang, Selangor, (Malaysia)*

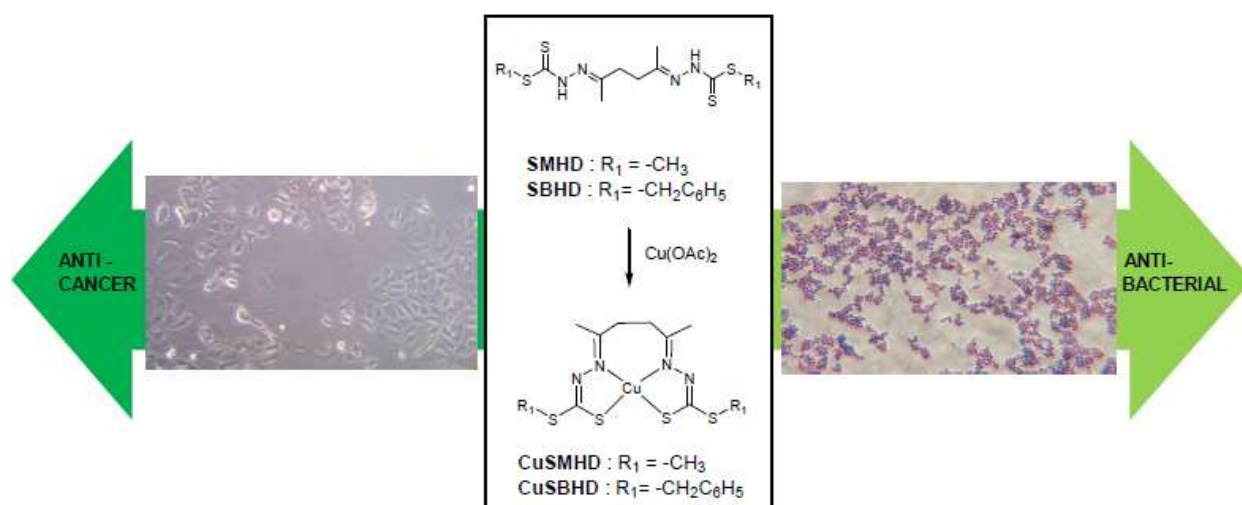
23 <sup>i</sup>*Department of Chemistry, Cape Breton University, Sydney, Nova Scotia B1P 6L2 (Canada)*

24  
25 **Keywords:** dithiocarbazate; Schiff base; macroacyclic ligand; tetradentate ligand; NNSS  
26 ligand; copper complexes; bioactivity; MDA-MB-231; MCF-7; Gram-positive; Gram-  
27 negative

28  
29 **Abstract**

30 Copper(II) complexes synthesized from the products of condensation of S-methyl- and S-  
31 benzyldithiocarbazate with 2,5-hexanedione (SMHDH2 and SBHDH2 respectively) have  
32 been characterized using various physicochemical (elemental analysis, molar conductivity,  
33 magnetic susceptibility) and spectroscopic (infrared, electronic) methods. The structures of  
34 SMHDH2, its copper(II) complex, CuSMHD, and the related CuSBHD complex as well as a  
35 pyrrole byproduct, SBPY, have been determined by single crystal X-ray diffraction. In order  
36 to provide more insight into the behaviour of the complexes in solution, electron  
37 paramagnetic resonance (EPR) and electrochemical experiments were performed.  
38 Antibacterial activity and cytotoxicity were evaluated. The compounds, dissolved in 0.5%  
39 and 5% DMSO, showed a wide range of antibacterial activity against 10 strains of Gram-  
40 positive and Gram-negative bacteria. Investigations of the effects of efflux pumps and  
41 membrane penetration on antibacterial activity are reported herein. Antiproliferation activity  
42 was observed to be enhanced by complexation with copper. Preliminary screening showed Cu  
43 complexes are strongly active against human breast adenocarcinoma cancer cell lines MDA-  
44 MB-231 and MCF-7.

## 45 TOC diagram



46

47

## 1. Introduction

Effective treatment of multi-drug resistant (MDR) bacterial infections has become increasingly challenging as the efficiency of the available antibiotic arsenal is reduced, resulting in increased frequency of therapeutic failure [1, 2]. Over-expression of efflux pumps can contribute to resistance of bacteria by expulsion of structurally unrelated compounds causing a decrease in the intracellular concentration of antibiotics [3, 4]. It is essential to understand efflux-mediated resistance in bacterial pathogens to develop efficient antibacterial agents circumventing this mechanism. In addition, parallel concerns relating to acquired drug resistance as well as the serious side-effects of anticancer drugs in the midst of the increasing rate of cancer diagnoses drives the effort to develop better alternatives [5, 6]. Due to their many tunable functionalities, dithiocarbamate compounds are exciting candidates for exploration and potential development as antimicrobial and cytotoxic agents.

Sulphur-nitrogen chelating agents derived from S-alkyl/aryl esters of dithiocarbamic acid have been extensively investigated in recent years for their cytotoxicity [7, 8], antibacterial [9], antiamebic [10], anti-*Trypanosoma cruzi* [11] and anti-*Mycobacterium tuberculosis* [12] activities. Considerable attention continues to be given to these and related Schiff bases [13-16], since their properties can be modulated by introducing different substituents through condensation of various S-substituted dithiocarbamate esters with a wide array of aldehydes and ketones. In many cases, the bioactivities of various dithiocarbamate derivatives have been shown to differ widely although there may be only slight modifications in their molecular structures [8]. Since these ligands possess both hard nitrogen and soft sulfur donor atoms they are capable of coordinating with a wide range of transition and non-transition metal ions forming metal complexes with interesting physicochemical and enhanced biological properties [17-19]. The wide diversity of structures displayed by macrocyclic and macroacyclic Schiff bases [20] results in various coordination abilities that could potentially lead to applications ranging from diagnostics to therapeutics [21-22]. As part of our ongoing exploration of these interesting properties, we investigated the synthesis and characterization of some macroacyclic bis(dithiocarbamate) Schiff bases and their Cu(II) complexes. Copper complexes derived from the analogues thiosemicarbazate have also been subjected to intensive research [23-26] and appear to be very efficient antimicrobial [27] and anticancer [28] agents. The copper(II) complexes of quadridentate NNSS donor ligands reported in the literature are also known to be neutral, stable ( $K_{\text{ass}}=10^{18}$ ) compounds that easily cross cellular

82 membranes [23, 29]. Thus, copper ion was a logical choice for complexation in our search for  
83 effective metallodrugs.

84

85 The main aim of the present work is to explore the biological potential of newly  
86 synthesized bis(dithiocarbazato) ligands and their Cu(II) complexes by determining their  
87 potencies against different bacterial strains expressing a multi-drug resistance phenotype and  
88 the effect of efflux pumps and membrane penetration on their antibacterial activity. In  
89 addition cytotoxicity assays against two breast cancer cell lines was carried out to determine  
90 the effect of complexation with copper upon the activity of the ligands against these cells.  
91 Whereas syntheses of many dithiocarbazate compounds have been reported in the literature,  
92 reports on the bioactivities [30], crystallography, EPR and electrochemistry [31, 32] of Cu(II)  
93 bis(dithiocarbazate) complexes are limited. To develop such compounds with effective  
94 pharmacological activity, it is essential to orient effort towards correlating the biological  
95 activities of this class of compounds with their solid and solution structures as well as their  
96 physicochemical properties to identify the optimum geometry about the Cu ion. This goal can  
97 be achieved through the synthesis of a graduated series of ligands designed to reveal the  
98 mode of bioaction.

99

100

101

102

103

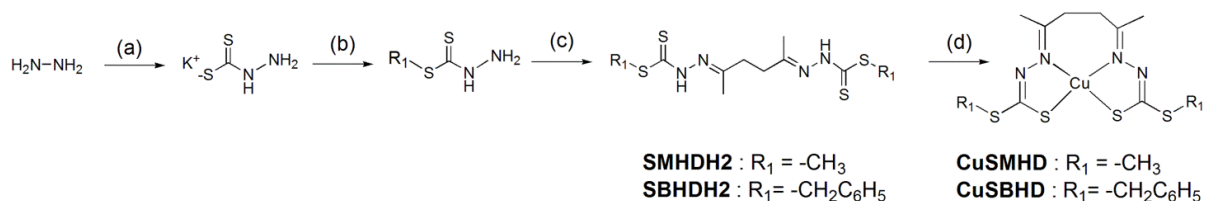
104

## 105 2. Results and Discussion

### 106 2.1. Synthesis and characterization

107 The synthesis of S-substituted dithiocarbazates was performed as previously  
108 described [33, 34]. Carbon disulfide and hydrazine were reacted in basic ethanol. After  
109 workup, the dithiocarbazate produced was directly reacted with methyl iodide or benzyl  
110 chloride to afford S-methyldithiocarbazate (SMDTC) and S-benzylthiocarbazate (SBDTC),  
111 respectively. Schiff bases were then prepared by a slight variation of the method described by  
112 Ali *et al.* [35]. The respective S-substituted dithiocarbazates and 2,5-hexanedione were  
113 condensed in 2:1 ratio (Scheme 1). The initial attempts to synthesize the ligand SBHDH2  
114 with prolonged heating followed by purification using column chromatography were  
115 unsuccessful. NMR, ESI, elemental analysis and single crystal X-ray diffraction confirmed  
116 cyclization to a pyrrole derivative. We postulate that bis(dithiocarbazate) indeed formed but  
117 was then hydrolyzed to mono(dithiocarbazate) and S-benzylthiocarbazate [36, 37] with  
118 subsequent cyclization of the mono(dithiocarbazate) to a pyrrole *via* the Paal-Knorr reaction.  
119 To our knowledge, this is the first pyrrole derived from a dithiocarbazate reported although  
120 there are two recent reports of formation of pyrrole byproducts upon reaction of  
121 thiosemicarbazone with 2,5-hexanedione [38, 39]. Encouraged by the remarkable  
122 pharmacological properties of functionalized pyrroles [40, 41], we tested the compound for  
123 its antimicrobial activity, the results of which are discussed below. The Schiff base,  
124 SBHDH2, was finally obtained using either of the following two methods: stirring the dione  
125 and SBDTC at room temperature for 30 minutes or heating for only 5 minutes after which the  
126 white precipitate formed immediately. SMHDH2 was synthesized without the complication  
127 of side-reaction occurrence. The precipitate was recrystallized to afford pure SMHDH2 (70%  
128 yield).

129  
130 Cu(II) complexes with NNSS coordination were obtained from the reaction of  
131 copper(II) acetate with an equimolar amount of the respective ligand (in acetonitrile for  
132 SBHDH2 and methanol for SMHDH2). The complexes were isolated by filtration with yields  
133 of 77% and 73% for CuSMHD and CuSBHD, respectively. Black crystals were grown from  
134 acetonitrile.



135

136 **Scheme 1.** Synthesis of the copper complexes derived from bis(dithiocarbazate) ligands. a)  
 137  $CS_2$ , KOH, EtOH,  $0^\circ C$ , 1 h; b)  $CH_3I$  or  $PhCH_2Cl$ , EtOH,  $0^\circ C$ , 5 h; c) for SMHDH2 (2,5-  
 138 hexanedione, EtOH,  $79^\circ C$ , 1 h), for SBHDH2 (2,5-hexanedione, EtOH,  $79^\circ C$ , 5 min) and d)  
 139 for CuSMHD [ $Cu(OAc)_2 \cdot H_2O$ , MeOH,  $65^\circ C$ , 1 h], for CuSBHD [ $Cu(OAc)_2$ , acetonitrile, r.t.,  
 140 1 h].

141

142

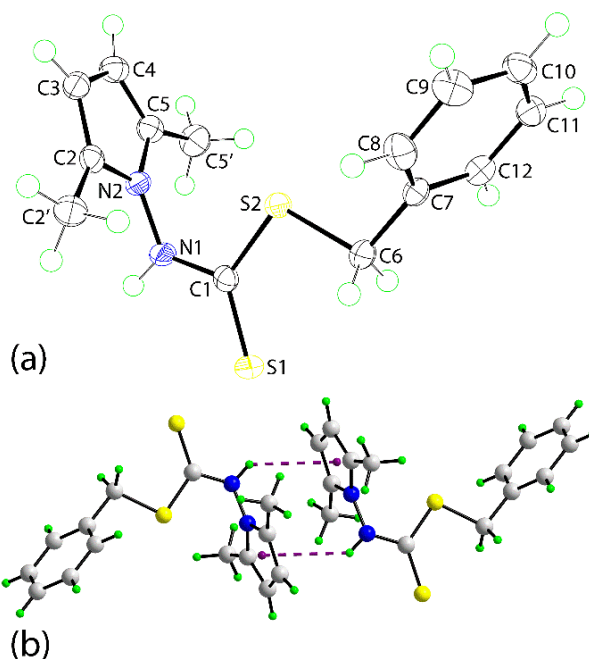
143 2.2. Characterization of the complexes in the solid state

144 The characteristic infrared bands of the S-substituted dithiocarbazate ligand,  $\nu(N-H)$   
 145 at *ca.*  $3129\text{ cm}^{-1}$  and  $\nu(C=S)$  at *ca.*  $1050\text{ cm}^{-1}$  disappeared upon formation of the Cu(II)  
 146 complexes. In addition,  $\nu(C=N)$  of the azomethine bond shifted to lower energy ( $1611\text{ cm}^{-1}$   
 147 and  $1606\text{ cm}^{-1}$  for CuSMHD and CuSBHD, respectively) and a second  $\nu(N=C)$  band in  
 148 complexes containing anionic dithiocarbazate moieties appeared [42]. The hydrazinic band,  
 149  $\nu(N-N)$ , at *ca.*  $828\text{ cm}^{-1}$  in the free ligand also shifted upon complexation, to higher  
 150 (CuSBHD) and lower (CuSMHD) wavenumbers. These observations confirm deprotonation  
 151 of the Schiff bases with coordination through the azomethine nitrogen atom. The  $\nu(CSS)$   
 152 band *ca.*  $985\text{ cm}^{-1}$  (ligand) splits into two components at  $1000\text{-}955\text{ cm}^{-1}$  upon complexation.  
 153 The presence of this band and the absence of the C=S band in the spectra of the metal  
 154 complexes provide additional evidence of the coordination of the Schiff base to the metal in  
 155 its thiolate form [43, 44]. To confirm the 1:1 stoichiometry, the complexes were also  
 156 characterized by elemental microanalyses for which the analytical data were found to agree  
 157 with the formulations proposed for the complexes. As expected for paramagnetic  $3d^9$  ions, the  
 158 magnetic susceptibility values measured at room temperature for the CuSMHD and CuSBHD  
 159 complexes (1.66 B.M and 1.48 B.M, respectively) suggest a square-planar environment (spin-  
 160 only value 1.73 B.M) [44, 45]. The slightly low values observed can be attributed to  
 161 interaction between Cu(II) ion centers [46, 47] or distortion in the Cu(II) environment [48].

162

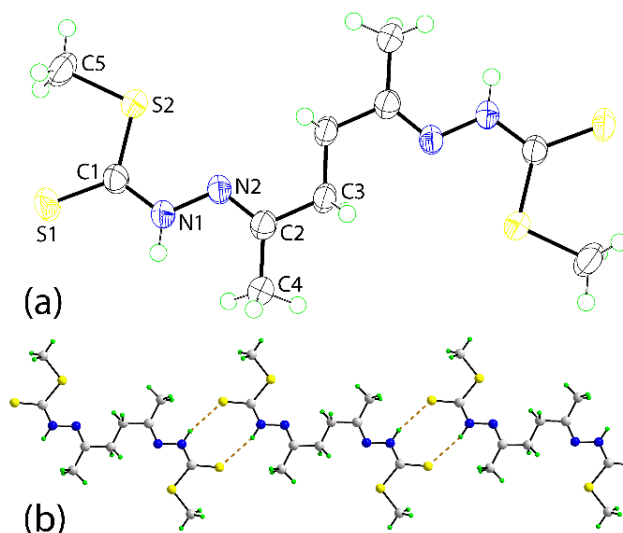
163 Crystals of SBPY, SMHDH2, CuSMHD and CuSBHD suitable for single crystal X-  
 164 ray diffraction were obtained; crystallographic data are given in Table 1. As mentioned in  
 165 Section 2.1, the pyrrolyl derivative, SBPY, is a cyclized product obtained during an attempted  
 166 synthesis of SBHDH2. The molecular structure of SBPY is shown in Fig. 1a. In SBPY, the

167 central  $\text{CN}_2\text{S}_2$  chromophore is planar (r.m.s. = 0.0490 Å) and forms dihedral angles of  
 168 88.49(4) and 68.14(4)° with the pyrrolyl and phenyl rings, respectively. As the rings lie to the  
 169 same side of the molecule, opposite to the thione-S1 atom, the overall conformation is best  
 170 described as being U-shaped. The dihedral angle between the rings is 60.874(6)° indicating a  
 171 splayed relationship. The thione-S1 and amine-H atoms are *syn* which might be expected to  
 172 lead to an eight-membered {...HNCS}<sub>2</sub> synthon in the crystal packing. Nevertheless, the  
 173 most prominent feature of the crystal packing is the formation of N–H... $\pi$  (pyrrolyl)  
 174 interactions, Fig. 1b, which lead to the formation of centrosymmetric dimeric aggregates.  
 175



176  
 177 **Fig. 1.** (a) The structure of SBPY, showing its atom-labelling scheme, and (b) the  
 178 supramolecular dimer sustained by N–H... $\pi$  (pyrrolyl) interactions.  
 179

180 SMHDH2 (Fig. 2) crystallises about a crystallographic centre of inversion located at  
 181 the mid-point of the C3–C3<sup>i</sup> bond indicating the molecule has an *anti* disposition of the  
 182 dithiocarbamate residues; symmetry operation *i*: 1–*x*, 2–*y*, 1–*z*. The conformation about the  
 183 hydrazone bond is *E*. The entire molecule is planar with the r.m.s. for the 18 non-hydrogen  
 184 atoms comprising the entire molecule being 0.038 Å, with the maximum deviations being  
 185 ±0.061 Å for the S2 atom.  
 186



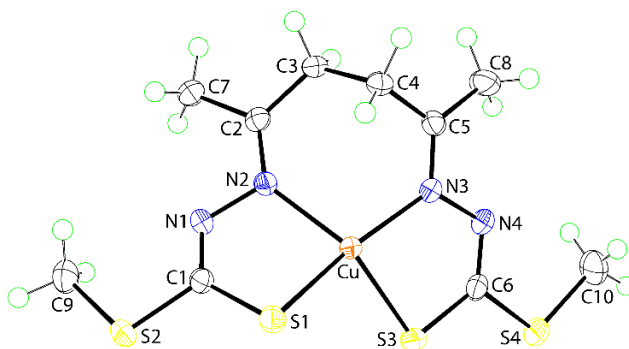
187

188 **Fig. 2.** (a) The structure of SMHDH2, showing its atom-labelling scheme. Unlabelled atoms  
 189 are related by the symmetry operation  $1-x, 2-y, 1-z$ , and (b) supramolecular chain mediated  
 190 by N–H...S hydrogen bonds via centrosymmetric eight-membered  $\{\dots\text{HNCS}\}_2$  synthons.  
 191  $[\text{N1}–\text{H1n}\dots\text{S1} = 2.64(2) \text{ \AA}$ ,  $\text{N1}\dots\text{S1} = 3.455(2) \text{ \AA}$ , and angle at H1n =  $156(3)^\circ$ ; symmetry  
 192 operation  $i: 2-x, 2-y, 2-z]$

193

194 The doubly deprotonated SMHD species functions as a tetradentate  $\text{N}_2\text{S}_2$  donor in its  
 195 complex with copper(II). The molecular structure of  $\text{CuSMHD}$  is shown in Fig. 3 and  
 196 selected geometric bond lengths ( $\text{\AA}$ ) and angles ( $^\circ$ ) for this,  $\text{CuSBHD}$ , and for SMHDH2 are  
 197 given in Table 2. To a first approximation, the seven-membered ring may be described as  
 198 having a half-chair conformation where the C4 atom lies  $0.9317(16) \text{ \AA}$  above the plane  
 199 defined by the Cu, N2, N3, C2, C3 and C5 atoms; r.m.s. =  $0.1373 \text{ \AA}$  with maximum  
 200 deviations  $0.1590(6) \text{ \AA}$  for Cu and  $-0.1595(10) \text{ \AA}$  for C2. The two five-membered chelate  
 201 rings have similar conformations. The S1-containing ring is an envelope with the flap atom,  
 202 Cu, lying  $0.7857(16) \text{ \AA}$  above the least-squares plane defined by the remaining four atoms  
 203 (r.m.s. =  $0.0119 \text{ \AA}$ ). The S3-containing ring is considerably more planar but can still be  
 204 described as having an envelope conformation with Cu being the flap atom. In this  
 205 description, the Cu atom lies  $0.2103(18) \text{ \AA}$  out of the plane defined by the four remaining  
 206 atoms which has a r.m.s. of  $0.0043 \text{ \AA}$ . There is a clear distortion away from the ideal square  
 207 planar geometry as is commonly observed in seven-membered rings having two hydrazone  
 208 bonds [49]. In  $\text{CuSMHD}$ , the angle between the two five-membered chelate rings is  $46.10(2)^\circ$   
 209 and the range of angles subtended at the Cu atom is  $84.89(3)^\circ$  for S1–Cu–N2 to  $164.90(4)^\circ$   
 210 for S1–Cu–N3.

211



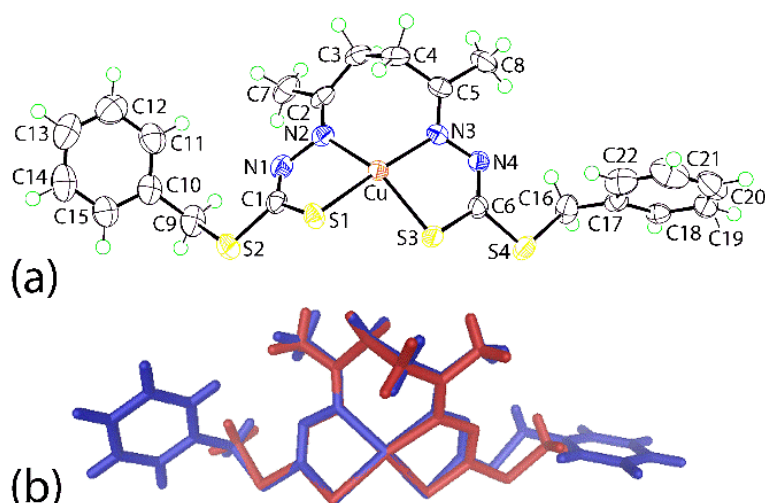
212  
213 **Fig. 3.** The structure of CuSMHD, showing its atom-labelling scheme.

214

215 The availability of the crystal structure of SMHDH2 enables a comparison of the  
216 geometric parameters in the free molecule and in its coordinated dianion in CuSMHD. Two  
217 quite distinct differences are noted in the bond lengths collected in Table 2. First and  
218 foremost, there has been a significant elongation, 0.08 Å, of the formally C1=S2 thione bond  
219 in SMHDH2 once this atom is complexed to Cu. Secondly, there has been a notable  
220 reduction, 0.05 Å, of the amine C1–N2 bond in SMHDH2, consistent with the formation of  
221 an imine bond in the complex. The reorganisation of electron density around the NCS<sub>2</sub>  
222 residue results in contraction of the S–C–S angle with concomitant expansion in the angles  
223 involving the double bonded nitrogen atom, Table 2. The crystal packing diagram reveals that  
224 the molecules stack in columns aligned along the b-axis with no directional interactions  
225 between them.

226 The molecular structure of CuSBHD (Fig. 4a and Table 2) shows the same features as  
227 CuSMHD, consistent with the notion that the nature of the S-bound substituent, methyl or  
228 benzyl, does not exert a significant effect upon the structure. This observation is highlighted  
229 in the overlay diagram shown in Fig. 4b. The seven-membered ring in CuSBHD has a half-  
230 chair conformation with the C4 atom lying 0.9970(19) Å above the plane defined by the Cu,  
231 N2, N3, C2, C3 and C5 atoms; r.m.s. = 0.2078 Å with maximum deviations 0.2432(7) Å, for  
232 Cu, and -0.3012(10) Å, for N3 indicating that this chelate ring is more distorted than in  
233 CuSMHD. The S1-containing five-membered chelate ring is an envelope with the flap atom  
234 being the Cu atom which lies 0.7703(19) Å above the least-squares plane defined by the  
235 remaining four atoms (r.m.s. = 0.0004 Å), as is the S3-chelate ring with the Cu atom lying  
236 0.423(2) Å above the plane of the four remaining atoms (r.m.s. = 0.0027 Å). In CuSBHD, the  
237 angle between the two five-membered chelate rings is 48.93(4)°, and the range of angles  
238 subtended at the Cu atom is 84.35(4)° for S3–Cu–N3 to 175.08(4)° for S1–Cu–N3, marginally  
239 broader than observed in CuSMHD, Table 2.

240



241

242 **Fig. 4.** (a) The structure of CuSBHD, showing its atom-labelling scheme, and (b) overlay  
 243 diagram of CuSMHD (red image) and CuSBHD (blue). The complex molecules are  
 244 overlapped so that the S1, Cu and S3 atoms are coincident.  
 245

246 The molecular packing of CuSBHD also resembles that of CuSMHD in that columns of  
 247 molecules are evident, aligned along the a-axis. However, the CuSBHD molecules are linked  
 248 by a combination of C–H...S and C–H... $\pi$  (phenyl) interactions. Geometric parameters  
 249 characterising the intermolecular interactions operating in the crystal structure of CuSBHD:  
 250 C4–H4a...S4<sup>i</sup> = 2.83 Å, C4...S4<sup>i</sup> = 3.7647(16) Å, and angle at H4a = 158° for i: -x, -1/2+y, -1/2-  
 251 z; C4–H4b...S3<sup>ii</sup> = 2.84 Å, C4...S3<sup>ii</sup> = 3.6946(19) Å, and angle at H4b = 145° for ii: -x, 1-y, -  
 252 z; C18–H18...S4<sup>iii</sup> = 2.86 Å, C18...S4<sup>iii</sup> = 3.6811(17) Å, and angle at H18 = 145° for iii: x,  
 253 1½-y, -1/2+z; C3–H3a...Cg(C17–C22)<sup>i</sup> = 2.89 Å, C3...Cg(C17–C22)<sup>i</sup> = 3.6538(17) Å, and  
 254 angle at H3a = 135°.

255

256 The four-coordinate structures described here for CuSBHD and CuSMHD, with the  
 257 dianions in the iminothiolate form, are consistent with literature precedents [15, 16, 49-52].  
 258

259 **Table 1**  
 260 Crystallographic and refinement details for SBPY, SMHDH2, CuSMHD and CuSBHD  
 261

262	Compound	SBPY	SMHDH2	CuSMHD	CuSBHD
263	Formula	C <sub>14</sub> H <sub>16</sub> N <sub>2</sub> S <sub>2</sub>	C <sub>10</sub> H <sub>18</sub> N <sub>4</sub> S <sub>4</sub>	C <sub>10</sub> H <sub>16</sub> CuN <sub>4</sub> S <sub>4</sub>	C <sub>22</sub> H <sub>24</sub> CuN <sub>4</sub> S <sub>4</sub>
264	Formula weight	276.41	322.52	384.05	536.23
265	Crystal colour/habit	Colourless plate	Yellow needle	Black prism	Black prism
266	Crystal dimensions/mm	0.04 x 0.20 x 0.21	0.03 x 0.06 x 0.24	0.04 x 0.12 x 0.18	0.11 x 0.22 x 0.28
267	Crystal system	monoclinic	triclinic	monoclinic	monoclinic
268	Space group	<i>P</i> 2 <sub>1</sub> / <i>c</i>	<i>P</i> 1	<i>C</i> 2/ <i>c</i>	<i>P</i> 2 <sub>1</sub> / <i>c</i>
269	<i>a</i> /Å	9.2991(4)	5.1646(5)	24.6441(8)	10.7937(1)
270	<i>b</i> /Å	15.9635(8)	7.2792(8)	7.9100(2)	18.8337(2)
271	<i>c</i> /Å	9.4848(5)	10.7840(12)	16.8972(6)	11.8412(2)
272	<i>α</i> /°	90	100.652(9)	90	90
273	<i>β</i> /°	96.155(1)	90.751(9)	111.167(4)	103.410(1)
274	<i>γ</i> /°	90	107.305(10)	90	90
275	<i>V</i> /Å <sup>3</sup>	1399.87(12)	379.39(7)	3071.62(18)	2341.51(5)
276	<i>Z</i>	4	1	8	4
277	<i>D<sub>c</sub></i> /g cm <sup>-3</sup>	1.312	1.412	1.661	1.521
278	<i>F</i> (000)	584	170	1576	1108
279	<i>μ</i> /mm <sup>-1</sup>	0.364	5.662	1.956	1.308
280	Measured data	19199	4869	19072	58909
281	Radiation	MoKα	CuKα	MoKα	MoKα
282	<i>θ</i> range/°	2.5–27.5	4.2–71.6	2.6–27.5	2.2–27.5
283	Unique data	3207	1455	3490	5353
284	Observed data ( <i>I</i> ≥ 2.0σ( <i>I</i> ))	2722	1197	3291	4827
285	<i>R</i> , obs. data; all data	0.032; 0.041	0.046; 0.055	0.019, 0.021	0.028, 0.032
286	<i>a</i> , <i>b</i> in weighting scheme	0.030, 0.621	0.078, 0.048	0.032, 2.432	0.050, 1.156
287	<i>R<sub>w</sub></i> , obs. data; all data	0.071; 0.075	0.121; 0.130	0.054, 0.055	0.077, 0.080
288	Residual electron density				
289	peaks/e Å <sup>3</sup>	0.30, -0.26	0.43, -0.28	0.37, -0.31	0.67, -0.47

290 **Table 2**

291 Selected geometric parameters (Å, °) for SMHDH2, CuSMHD and CuSBHD

292	293			
294	<b>SMHDH2</b>	<b>CuSMHD</b>	<b>CuSBHD</b>	
295	296			
296	Parameter			
297	Cu–S1	–	2.2480(4)	2.2458(4)
298	Cu–S3	–	2.2523(4)	2.2659(4)
299	Cu–N2	–	2.0555(12)	2.0704(13)
300	Cu–N3	–	1.9792(12)	1.9927(14)
301	C1–S1, S2	1.655(3), 1.763(3)	1.7373(14), 1.7579(14)	1.7354(16), 1.7573(17)
302	C6–S3, S4	–	1.7380(14), 1.7533(14)	1.7404(16), 1.7560(16)
303	N1–C1, N2–C2	1.339(3), 1.281(3)	1.2892(19), 1.2914(18)	1.286(2), 1.292(2)
304	N1–N2	1.391(3)	1.4182(16)	1.4181(18)
305	C5–N3, C6–N4	–	1.2872(18), 1.2887(18)	1.285(2), 1.286(2)
306	N3–N4	–	1.4073(16)	1.4019(18)
307	S1–Cu–S3	–	92.795(14)	91.655(15)
308	S1–Cu–N2	–	84.89(3)	85.26(4)
309	S1–Cu–N3	–	164.90(4)	175.08(4)
310	S3–Cu–N2	–	148.04(3)	148.89(4)
311	S3–Cu–N3	–	85.76(4)	84.35(4)
312	N2–Cu–N3	–	104.21(5)	99.65(5)
313	C1–N1–N2	119.2(2)	113.22(11)	113.38(12)
314	C2–N2–N1	117.0(2)	112.01(11)	112.92(13)
315	C5–N3–N4	–	115.20(11)	115.88(13)
316	C6–N4–N3	–	112.83(11)	112.70(12)
317				
318	S1–C1–S2	123.83(16)	113.87(8)	111.63(9)
319	N1–C1–S1	122.7(2)	127.49(11)	128.34(13)
320	N1–C1–S2	113.51(18)	118.63(11)	120.01(12)
321	S3–C6–S4	–	113.94(8)	113.16(9)
322	N4–C6–S3	–	127.17(11)	126.59(12)
323	N4–C6–S4	–	118.89(10)	120.23(12)
324				

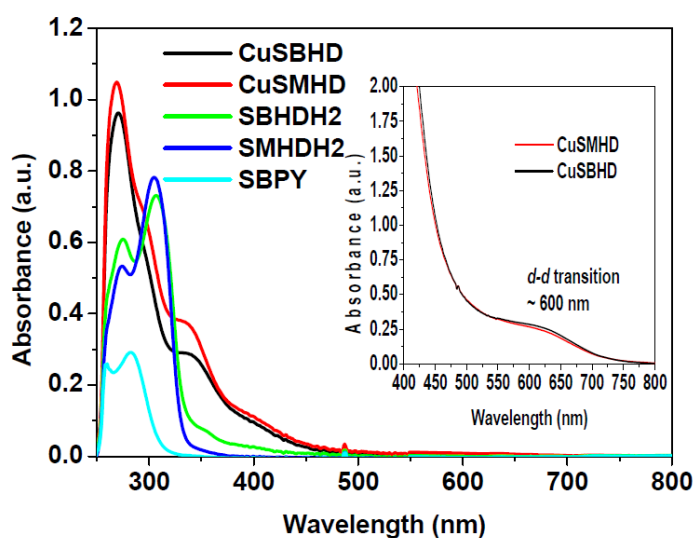
325

326

## 327 2.3. Solution characterization of the complexes

328 The UV-Vis absorption spectra of the compounds in DMSO (25  $\mu\text{M}$  and 1 mM) are  
 329 given in Figure 5. Both complexes showed  $\pi \rightarrow \pi^*$  and  $n \rightarrow \pi^*$  intra-ligand transitions at 272  
 330 nm, 295 nm and 338 nm and a  $d-d$  band at approximately 600 nm that can be attributed to  
 331 Jahn-Teller distortion from square planar geometry [47]. The presence of the S  $\rightarrow$  Cu(II)  
 332 LMCT band at  $\sim 400$  nm in the spectra of both metal complexes is strong evidence that the  
 333 metal ion is coordinated to sulphur [43, 53].

334



335

336 **Fig. 5.** UV-Vis spectra for all compounds (25  $\mu\text{M}$ , DMSO). The insert shows the  $d-d$  band of  
 337 the Cu complexes (1 mM solutions).

338

339 That the ligands and their corresponding complexes be stable at physiological pH is  
 340 an important prerequisite for evaluation of their biological activity. The molar conductance  
 341 values for the complexes in DMSO were in the range  $12-13 \Omega^{-1} \text{ cm}^2 \text{ mol}^{-1}$ , indicating that  
 342 there is essentially no dissociation in that solvent [54]. To more precisely evaluate their  
 343 stability, reverse phase HPLC experiments were performed. The ligands and their complexes  
 344 were eluted on a C18-column with a gradient increase in concentration of  $\text{CH}_3\text{CN}$  in  $\text{H}_2\text{O}$   
 345 (from 5% to 100% over 30 min), containing 0.1 % TFA to maintain pH. The compounds were  
 346 detected at 220 and 280 nm. The chromatograms of the purified ligands showed three peaks  
 347 that could correspond to the expected ligand, the hydrolyzed hydrazone and the pyrrole  
 348 byproduct whereas the complexes showed only the single peak of the copper complexes (see  
 349 Supplementary Data). It is noteworthy that the hydrazone bond stability significantly  
 350 increased upon metal-complexation under acidic conditions suggesting that complexation

351 could be used as a means to protect the ligand from degradation that might occur in biological  
352 systems before free ligand could reach its target.

353

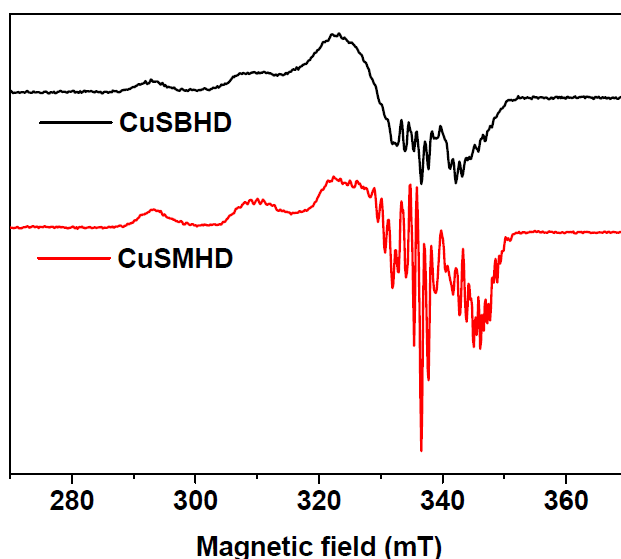
#### 354 2.4. Electron Paramagnetic Resonance (EPR)

355 The EPR spectra recorded in DMF (Figure 6) are typical of distorted square planar  
356 Cu(II) complexes having axial symmetry with the unpaired electron mainly in the  $d_{x^2-y^2}$   
357 orbital. The spectra also exhibit partially resolved superhyperfine features. The  $g_{\parallel}$  values for  
358 all the complexes are similar to those previously reported for analogous Cu(II)N<sub>2</sub>S<sub>2</sub>  
359 complexes [16, 24, 55]. Kivelson and Nieman [56, 57] suggested that  $g_{\parallel}$  values higher than  
360 2.3 are indicative of a predominantly ionic character for metal-ligand bonds, whereas  $g_{\parallel}$   
361 values smaller than 2.3 reveal metal-ligand bonds of predominantly covalent character, as is  
362 the case here (see Table 3). In addition, the relatively small  $g_{\parallel}$  value (~2.20) suggests a strong  
363 nitrogen character in the singly occupied molecular orbital. The equation below [42, 58] was  
364 used to calculate the molecular orbital coefficients,  $\alpha^2$  (in-plane  $\sigma$ -bonding):

$$365 \quad \alpha^2 = (A_{\parallel} / 0.036) + (g_{\parallel} - 2.0036) + 3 / 7 (g_{\perp} - 2.0036) + 0.04$$

366 An  $\alpha^2$  value of 0.5 indicates complete covalent bonding, while 1.0 suggests complete ionic  
367 bonding. The observed value of 0.64 for the present complexes is evidence that these copper  
368 complexes have some covalent character, as suggested above. EPR spectroscopy is sensitive  
369 to angular distortions at the Cu(II) centre, particularly those involving distortions from planar  
370 to tetrahedral geometry which generally result in a decrease in  $A_{\parallel}$  and an increase in  $g_{\parallel}$  [53].  
371 The empirical factor  $f (= g_{\parallel}/A_{\parallel})$  [59, 60] is a measure of deviation from idealized geometry. Its  
372 value ranges between 105 and 135 cm for square planar complexes, depending on the nature  
373 of the coordinated atoms, while, for tetrahedral structures, values from 160 to 242 cm suggest  
374 a moderate to considerable tetrahedral distortion. In solution as well as in the solid, CuSBHD  
375 displays a slightly higher degree of tetrahedral distortion than CuSMHD. Both are slightly  
376 more distorted than analogues, probably due to their extended carbon backbones [16, 24, 55].

377



378

379 **Fig. 6.** EPR spectra of CuSBHD and CuSMHD recorded at a microwave frequency 9.50  
 380 GHz, power 0.25 mW, modulation amplitude 0.2 mT, modulation frequency 100 kHz, and  
 381 time constant 164 ms, at 50 K. Samples were prepared in DMF (1 mM).

382

### 383 Table 3

384 EPR parameters measured from the spectra of CuSBHD and CuSMHD in DMF

385

	$g_{\parallel}$	$g_{\perp}$	$A_{\parallel}^{[a]}$	$f^{[b]}$	$\alpha^2$
CuSMHD	2.15	2.06	460 (153)	141	0.64
CuSBHD	2.16	2.05	451 (150)	143	0.64

386

[a] MHz ( $\times 10^4 \text{ cm}^{-1}$ ) [b] cm

387

## 388 2.5. Electrochemistry

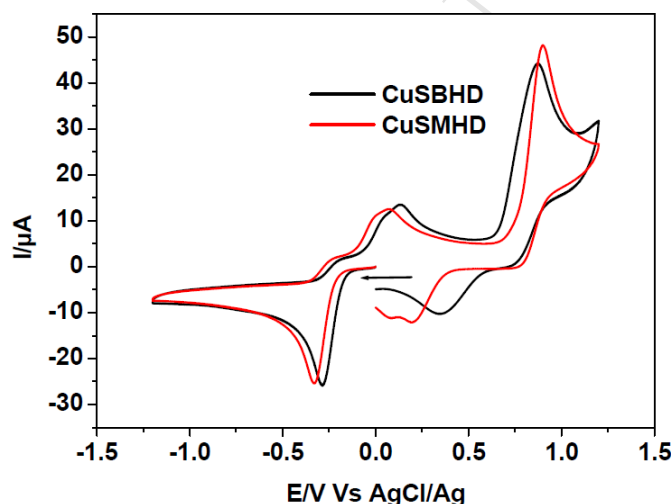
389 As redox properties have been linked to SOD and anticancer properties of metal  
 390 complexes [61, 62], we describe herein the electrochemical properties of Cu(II) bis(dithio  
 391 carbazate). Figure 7 shows the profile of the Cu(II) complexes obtained with SMHDH2 and  
 392 SBHDH2 at scan rate  $100 \text{ mV s}^{-1}$ . Both complexes undergo an irreversible one-electron  
 393 reduction at  $E_{pc} = -0.328$  and  $-0.285 \text{ V}/(\text{AgCl}/\text{Ag})$  and  $\text{Fc}^+/\text{Fc} = 0.563 \text{ V}$ , respectively,  
 394 coupled with oxidation at  $E_{pa} = 0.069$  and  $0.129 \text{ V}/(\text{AgCl}/\text{Ag})$ . These waves can be assigned  
 395 to the irreversible oxidation/reduction of Cu(II)/Cu(I) [52]. The ligands were found to be  
 396 redox innocent. The irreversible nature of the copper-centered redox waves contrasts with the  
 397 quasi-reversible reduction previously reported for CuATSM and CuAATSM analogues [50,

398 51]. The loss of reversibility observed in this work is most likely related to differences in the  
399 geometric rearrangement about the Cu(II)/Cu(I) ions in this ligand system with two carbon  
400 atoms between the two hydrazone functions. The Cu(II)/Cu(I) redox potentials of CuSMHD  
401 and CuSBHD are also more positive than those reported for previous examples. The ease of  
402 deformation seems to favour reduction. The difference in redox potential between CuSMHD  
403 and CuSBHD may be rationalized by induction due to the stronger electron-donating effect of  
404 the methyl group compared to benzyl [63].

405

406 As mentioned above, the oxidation proceeding at higher positive potential has  
407 previously been assigned to the copper(III/II) redox couple. It is interesting to note the  
408 occurrence of an additional peak, which can be attributed to the reduction of a species  
409 produced by the second oxidation. However, the nature of this oxidized complex has not been  
410 determined.

411



412

413 **Fig. 7.** Cyclic voltammograms of the Cu complexes (1.7 mM) in anhydrous deoxygenated  
414 DMF containing 0.1 M tetrabutylammonium hexafluorophosphate as the supporting  
415 electrolyte. Working electrode: glassy carbon; counter electrode: Pt wire; reference electrode:  
416 AgCl/Ag, scan rate: 100 mV/s. All sweeps were initiated in the direction of the arrow.

417 **Table 4**

418 Electrochemical data for CuSMHD and CuSBHD vs AgCl/Ag.

419

	Cu(II)/Cu(I)		Cu(III)/Cu(II)	
	$E_{pc}/V$	$E_{pa}/V$	$E_{pc}/V$	$E_{pa}/V$
CuSMHD	-0.328	0.069	0.195	0.899
CuSBHD	-0.285	0.129	0.357	0.870

420

421 **Biological evaluation**422 *3.1. Antibacterial activity*

423 The free Schiff bases and their metal complexes were tested for their ability to inhibit  
 424 the growth of ten strains of Gram-negative and Gram-positive bacteria (Table 5). The effects  
 425 of a membrane permeabilizing agent and efflux pumps were investigated in an attempt to  
 426 correlate the activity of the compounds with their penetration into the bacteria and the  
 427 resistance mechanisms of the bacteria.

428

429 One of the limitations of this class of compounds is their poor solubility in aqueous  
 430 solution. The universal solvent DMSO has been used in many studies to pre-dissolve the  
 431 compounds for biological assays. However, it has been shown that DMSO solutions (1% to  
 432 10%) considerably affect the growth of fungi and cancerous cells, and, at 15%, DMSO  
 433 effectively eliminates the growth of certain bacteria [64-66]. DMSO has also been reported to  
 434 decrease membrane rigidity, thus facilitating membrane diffusion of exogenous species [67-  
 435 70]. As DMSO is used in this work to encourage dissolution of the compounds and since  
 436 there is no rule of thumb for the amount of DMSO to be used for antibacterial assay, it was  
 437 essential to examine the influence of DMSO concentrations on the growth curve of the  
 438 selected bacterial strains. The minimum inhibitory concentration (MIC) values were  
 439 determined at 0.5% and 5% (v:v) DMSO. We found that the growth of *A. baumannii* and *P.*  
 440 *aeruginosa* is inhibited by DMSO at a concentration of only 5% thus preventing  
 441 determination of MIC at this concentration. The growth of *E. coli* and *E. aerogenes* (see  
 442 Supplementary Data) was also affected by DMSO at 5%. Differences were observed between  
 443 MIC values against the mutated strains *E. coli* AcrAB- and *E. aerogenes* 298 TolC- obtained  
 444 in the presence of 0.5% or 5% DMSO for certain molecules, in particular, CuSMHD.  
 445 Additional MIC values determined for CuSMHD using DMSO 50%, 30% and 20% (2.5%,

446 1.5% and 1% final v:v DMSO) were all higher than 128  $\mu\text{M}$  while with 5% of DMSO, the  
447 MIC values were in the range of 1-2 and 0.5-1  $\mu\text{M}$  against *E. coli* AcrAB- and *E. aerogenes*  
448 298 TolC-, respectively. Because of the effect of DMSO on bacterial growth, we are unable to  
449 confirm whether the value truly reflects the specific antimicrobial activity of the tested  
450 compound and not a synergetic effect involving the compound and DMSO. MIC values  
451 recorded using 0.5% DMSO are used for discussion of the role of membrane permeabilizing  
452 agents and efflux pumps since DMSO at this concentration was shown not to interfere with  
453 bacterial growth.

454

455 Since it has been reported that low permeability of the outer membrane and the  
456 efficiency of efflux pumps [3, 4] are prime factors limiting intracellular activity of potential  
457 antimicrobial compounds, it is expected that the presence of a substance known to increase  
458 membrane permeability, such as polymyxin B nonapeptide (PMBN) [71], would act  
459 synergistically to improve uptake of the compounds under study and consequently would  
460 affect their antimicrobial efficiency in a positive manner. The compounds were tested in the  
461 presence and absence of sub-inhibitory concentrations (1/5 of the MIC value) of PMBN. In  
462 the absence of PMBN only SMHDH2 was active against the strains tested (MIC  $\geq$  64  $\mu\text{M}$ ).  
463 SMHDH2 showed moderate activity against *S. aureus*. However, up to 3-fold improvement  
464 in activity (MIC values) was observed for the organic compounds SMHDH2, SBHDH2 and  
465 SBDP in the presence of PMBN against both Gram-negative and Gram-positive bacteria.  
466 These results imply that apparent lack of activity was due to the inability of the compounds to  
467 efficiently permeate the bacterial membrane. SMHDH2 showed a broad range of moderate  
468 activity against various strains. It was most effective against *E. coli* AcrAB-, *A. baumannii*, *P.*  
469 *aeruginosa* and *S. aureus* (MIC values  $\sim$ 16  $\mu\text{M}$ ), thus making it a potential antimicrobial  
470 agent in the presence of PMBN. These results are not unexpected since many previous  
471 reports have shown that the biological activity of dithiocarbazato compounds can be greatly  
472 modified by the presence of different substituents. The enhanced activity observed for  
473 SMHDH2 compared to its S-benzyl analog is consistent with the observation that the Schiff  
474 base prepared from 2-benzoylpyridine with S-methyldithiocarbazate (SMDTC) was a highly  
475 effective inhibitor of *E. coli* and *S. aureus* whereas that prepared with the S-  
476 benzylidithiocarbazate (SBDTC) analog showed no activity [72].

477

478 **Table 5**  
 479 Antibacterial activity.  
 480

Compound	Minimum Inhibitory Concentration (MIC) ( $\mu\text{M}$ )																		
	Gram-										Gram+								
	<i>E. coli</i>				<i>E. aerogenes</i>				A. baumannii		K. pneumoniae		<i>P. aeruginosa</i>		<i>S. enterica</i>		<i>S. aureus</i>		
	AG100 WT		AG100A AcrAB-		EA289 AcrAB+		EA294 AcrAB-		EA298 TolC-		ATCC 19606		ATCC 11296		PA01		SL696		SA1199
% DMSO	0.5	5	0.5	5	0.5	5	0.5	5	0.5	5	0.5	5	0.5	5	0.5	5	0.5	5	
SMHDH2	>128	>128	>128	>128	>128	128-64	>128	64	>128-128	>128	64	128	64	128-64	>128	>128	32	64-32	
+PMBN	32	32	16	16	>128-128	64	128-32	64	128	32	16	64	32-16	16-8	64	32	32-16	64-32	
CuSMHD	>128	>128	>128	>128	>128	>128	>128	>128	>128	>128	>128	>128	>128	>128	>128	>128	>128	>128	
+PMBN	>128	>128	>128	1-2	>128	>128	>128	>128	>128-128	0.5-1	>128	>128	>128	>128	>128	>128	>128	>128	
SBHDH2	>128	128	>128	128	>128	128-64	>128	64	>128-128	64	>128	>128	128	>128	>128	>128	>128	64-32	
+PMBN	>128	64	128-32	32-16	>128-128	64	>128-64	64	>128-64	16-4	128-64	128-64	32-16	64-32	>128	64	16	128	
CuSBHD	>128	>128	>128	>128	>128	>128	>128	>128	>128	>128	>128	>128	>128	>128	>128	>128	>128	>128	
+PMBN	>128	>128	>128	>128	>128	>128	>128	>128	>128	>128	>128	>128	>128	>128	>128	>128	>128	>128	
SBPY	>64	>64	>64	>64	>64	>64	>64	>64	>64	>64	>128	>128	>128	>128	>128	>128	128	128-64	
+PMBN	64	64	32	16	>64	64	32	4	32	4	>128-128	>128	64	>128-128	64	64-32	128-64	128	
Cu(Ac) <sub>2</sub>	>128	>128	>128	>128	>128	>128	>128	>128	>128	>128	>128	>128	>128	>128	>128	>128	>128	>128	
+PMBN	>128	>128	>128	>128	>128	>128	>128	>128	>128	>128	>128	>128	>128	>128	>128	>128	>128	>128	

481  
 482 Colour code: MIC values or average MIC values  $\geq 64 \mu\text{M}$  = red,  $\leq 10 \mu\text{M}$  = green, in between  $64 \mu\text{M}$  and  $10 \mu\text{M}$  = colourless. MIC values  
 483 higher than  $64 \mu\text{M}$  indicate poor activity.

484 The role of efflux pumps was investigated using pump-deleted strains of Gram-negative  
485 *E. coli* and *E. aerogenes*. Both SMHDH2 and SBPY seemed more active (16  $\mu\text{M}$  and 32  $\mu\text{M}$ ,  
486 respectively) towards the isogenic strain in which the AcrAB pump was deleted as compared  
487 to wild-type *E. coli*. No significant activity was observed for SMHDH2 in the presence or  
488 absence of efflux pump for *E. aerogenes*. SBPY, on the other hand, showed differences in the  
489 MDR clinical isolate EA289 over expressing AcrAB efflux pump and on its AcrAB- and  
490 TolC- derivatives, EA294 and EA298, with improvement in MIC from  $> 64 \mu\text{M}$  to 32  $\mu\text{M}$ .  
491 These results confirmed that SBPY and SMHDH2 are recognized by the efflux pumps and  
492 expelled from the bacteria, thus limiting their bioactivity. Both SMHDH2 and SBHDH2  
493 showed activity towards Gram-positive *S. aureus*. Typically, antibacterial molecules are more  
494 active toward Gram-positive than Gram-negative bacteria [73, 74], because the additional  
495 outer membrane of the latter organisms impairs or slows down the drug uptake. It has often  
496 been reported in the literature that bioactivity of a ligand is enhanced by metal complexation  
497 [49, 60], but in our case, the formation of the copper complexes induces a loss of antibacterial  
498 potency of the compounds. A similar loss in activity was previously reported for  
499 palladium(II) and platinum(II) complexes of acetone Schiff bases [7]. This can be explained  
500 by the lower solubility of the metal complexes or by the lower stability of the hydrazone  
501 moiety in the case of the free ligands. As noted above, hydrolysis of the ligands occurring in  
502 aqueous solution at specific pH, may lead to reactive products that can be responsible for the  
503 toxicity. Since these observations strongly suggest that enhancement of antibacterial activity  
504 can be expected as a result of increasing solubility and membrane diffusion, efforts are  
505 currently being made to significantly improve the aqueous solubility of these compounds.

506

### 507 3.2. Cytotoxic assay

508 Cytotoxicity was evaluated *in vitro* against two breast cancer cell lines MDA-MB-231  
509 (human breast carcinoma cells not expressing nuclear estrogen receptors) and MCF-7 (human  
510 breast carcinoma cells expressing nuclear estrogen receptors). Measurements were carried out  
511 using MTT assay [75] which is based on the metabolic reduction of tetrazolium salt to form  
512 water insoluble formazan crystals. DMSO was used as a negative control in the assay. There  
513 was no perceptible precipitation of the compounds. The concentrations required to inhibit the  
514 growth of cancer cells by 50% ( $\text{IC}_{50}$ ) are given in Table 6.

515

516

517 **Table 6**

518 Cytotoxic assay results.

519

	IC <sub>50</sub> (μM)	
	MCF-7	MDA-MB-231
SMHDH2	138.90	9.61
SBHDH2	9.69	1.05
CuSMHD	2.60	2.34
CuSBHD	1.49	0.71
Tamoxifen	11.20	13.40

520

521 Both ligands displayed at least 9-fold better toxicity towards MDA-MB-231, indicating  
 522 that ligand toxicity is not only mediated by nuclear estrogen receptors. The stronger toxicity  
 523 exhibited by SBHDH2 may be related to facilitated diffusion into cells resulting from its  
 524 comparatively higher lipophilicity [12]. Complexation of the Schiff base ligands with  
 525 copper(II) has been found to produce synergistic effects on the antiproliferative activities of  
 526 some parent ligands [76] and here the complexes showed a marked cytotoxicity with IC<sub>50</sub>  
 527 values < 5.0 μM towards both cell lines. Like the ligands, the complexes are also more active  
 528 towards MDA-MB-231 cells, suggesting that their toxicity does not involve estrogen  
 529 receptors. For both cell lines, the benzyl substituted complex CuSBHD showed slightly  
 530 higher IC<sub>50</sub> values. Although a definitive structure-activity relationship cannot be deduced  
 531 since only a limited number of compounds was tested, observations indicate that the  
 532 enhanced activity of CuSBHD may be linked to higher cellular uptake resulting from  
 533 increased lipophilicity as suggested above for the ligand. Redox potential may also be a  
 534 discriminating factor since its higher redox potential means that reduction of Cu(II) is easier,  
 535 and consequently a higher content of Cu(I) could be generated. Cu(I) is prone to participate in  
 536 Fenton-type reactions that produce reactive oxygen species (ROS), which can damage  
 537 biomolecules within cells [62].

538

539 **4. Conclusions**

540 This study provides new insight into the structural, electrochemical and biological aspects  
 541 of macroacyclic Cu(II) complexes derived from S-substituted dithiocarbamate. All the  
 542 compounds exhibited good cytotoxicity toward MDA-MB-231 and MCF-7 breast cancer cell  
 543 lines. Their low antibacterial activity can be related to poor bacterial penetration and limited  
 544 solubility, both of which should be amenable to improvement by further functionalization of

545 the ligands. The anticancer activity of the ligands was enhanced by complexation with Cu(II).  
546 Expanding the carbon backbone between the hydrazone moieties resulted in further distortion  
547 from square planar geometry in both the solid state and in solution as well as a positive shift  
548 in the Cu(II)/Cu(I) reduction potential. A higher reduction potential could be related to the  
549 production of reactive oxygen species resulting in the enhanced bioactivity observed in this  
550 present work. Taking into consideration the serious side effects and the poor efficacy of  
551 clinical reference drugs, as well as the appearance of resistance during treatment, these  
552 complexes are potentially useful lead candidates for the development of new therapeutic  
553 agents to treat cancer and bacterial infections. In addition, this work underlines the need to  
554 consider the concentration of DMSO used to dissolve compounds, since DMSO may pre-  
555 sensitize the bacterial cells to the tested compounds. Reduced uptake of compounds due to  
556 low permeability of the outer cell membrane and the efficiency of efflux pumps were also  
557 shown to be issues to be addressed in subsequent studies. With these considerations in mind,  
558 our group is attempting to improve antimicrobial and anticancer activities of compounds in  
559 this family by exploring the design and synthesis of a new generation of S-substituted  
560 dithiocarbamate derivatives and their metal complexes.

## 561 **5. Experimental**

### 562 *5.1. Materials-instrumentation-physical measurements*

563 All chemicals and solvents were of analytical grade and were used as received.  
564 Chemicals: Potassium hydroxide (Merck), hydrazinium hydroxide (Merck), carbon disulfide  
565 (Sigma Aldrich), 2,5-hexanedione (Merck), and copper(II) acetate monohydrate (Analar). The  
566 IR spectra were recorded in the range of 550-4000  $\text{cm}^{-1}$  on a Perkin-Elmer 100 series FT-IR  
567 spectrophotometer in ATR mode. Magnetic susceptibility was measured with a Sherwood  
568 MSB-AUTO instrument at room temperature. All susceptibilities were corrected for the  
569 diamagnetic contribution using Pascal's constant. Microanalyses were carried out using either  
570 a LECO CHNS-932 analyzer or performed at the CNRS (Gif-sur-Yvette and Vernaison,  
571 France). The molar conductance of a  $10^{-3}$  M solution of each metal complex in DMSO was  
572 measured at 29°C using a Jenway 4310 conductivity meter and a dip-type cell with platinized  
573 electrode. The UV-Vis spectra were recorded on a Cary 300 Bio spectrophotometer (200-800  
574 nm) or Perkin Elmer Lambda 45 with a 1 cm optical path quartz cuvette.  $^1\text{H}$  NMR and  $^{13}\text{C}$   
575 NMR spectra were recorded using Bruker DRX300 spectrometers. The chemical shifts  
576 ( $\delta/\text{ppm}$ ) were calibrated relative to residual solvent signals. Electrospray-ionization mass

577 spectra (ESI-MS) were recorded with a Finnigan Mat 95S in the BE configuration at low  
578 resolution. Electron paramagnetic resonance (EPR) spectra were recorded on an X-band  
579 Bruker Elexsys 500 spectrometer equipped with a continuous flow helium cryostat (Oxford  
580 Instruments) and a temperature control system. The field modulation frequency was 100 kHz.  
581 The spectra were all recorded under nonsaturating conditions. Cyclic voltammetry (CV)  
582 measurements were recorded under argon using a 620C electrochemical analyzer (CH  
583 Instruments, Inc). The working electrode was a glassy carbon disk; a Pt wire was used as  
584 counter electrode and the reference electrode was AgCl/Ag. Immediately before  
585 measurements were taken, the working electrode was carefully polished with alumina  
586 suspensions (1, 0.3 and 0.05  $\mu\text{m}$ , successively), sonicated in an ethanol bath and then  
587 carefully washed with ethanol. Test solutions were prepared using 100  $\mu\text{L}$  of the complexes  
588 in anhydrous deoxygenated DMF (0.01 M) with 0.5 mL of tetrabutylammonium  
589 hexafluorophosphate (0.1 M) as the supporting electrolyte (total volume 0.6 mL). Ferrocene  
590 was used as internal reference: the ferrocinium/ferrocene one-electron redox process occurs  
591 at  $E_{1/2} = 0.508$  V (DMF) vs AgCl/Ag with scan rate = 0.1 V/s. RP-HPLC analysis was carried  
592 out using a Waters HPLC system that consisted of a combination of a dual wavelength UV-  
593 Vis absorbance detector (Waters 2487) and a binary pump (Waters 1525) equipped with an  
594 analytical cell for reaction monitoring or purity checking connected to Breeze software.  
595 Analytical HPLC measurements were performed using an ACE C18 column ( $250 \times 4.5\text{mm}$ )  
596 packed with spherical 5  $\mu\text{m}$  particles of 300  $\text{\AA}$  pore size. Experiments were carried out at a  
597 flow rate of 1  $\text{mL min}^{-1}$  at room temperature. Injection volume was 50  $\mu\text{L}$ . Sample  
598 concentration was approximately 1  $\text{mg mL}^{-1}$ .

599

## 600 5.2. Preparation of ligands and metal complexes

### 601 5.2.1 Synthesis of SBHDH2

602 A modification of the method described by Ali *et al.* [35] was used to synthesize  
603 SBHDH2. 2,5-Hexanedione (0.587 mL, 0.005 mol) was added to a hot solution of S-  
604 benzyldithiocarbamate (1.983 g, 0.01 mol) in absolute ethanol (150 mL) and the mixture was  
605 further heated for 5 min. The white precipitate formed was immediately filtered off, washed  
606 with cold ethanol and dried *in vacuo* over silica gel to yield the expected Schiff base (yield  
607 0.997 g, 42%). Elemental analysis for  $\text{C}_{22}\text{H}_{26}\text{N}_4\text{S}_4$ : Calc. C 55.66, H 5.52, N 11.80; Found C  
608 54.79, H 5.59, N 11.75.  $^1\text{H}$  NMR (300 MHz, DMSO- $d_6$ )  $\delta$  12.18 (s, 2H), 7.39 -7.20 (m,  
609 10H), 4.40 (s, 4H), 1.96 (s, 6H).  $^{13}\text{C}$  NMR (75 MHz, DMSO- $d_6$ )  $\delta$  197.16, 158.26, 137.15,  
610 129.15, 128.41, 127.05, 37.56, 34.05, 17.74. IR:  $\nu$  ( $\text{cm}^{-1}$ ) = 3147 (m, b), 1640 (w), 1054 (s),

611 981 (m), 828 (m). UV-Vis in DMSO:  $\lambda_{\max}$  nm ( $\log \epsilon$  in  $\text{L mol}^{-1} \text{cm}^{-1}$ ) = 276 (4.32), 308 (4.41),  
612  $\approx 360$  (3.32, sh). RP-HPLC:  $R_T$  (min) = 15.3, 18.3, 22.4. Molar conductivity:  $\Lambda$  ( $\text{ohm}^{-1}$   
613  $\text{cm}^2 \text{mol}^{-1}$ ) = 6.86.

614

### 615 5.2.2 Synthesis of SMHDH2

616 2,5-Hexanedione (0.587 mL, 0.005 mol) was added to a solution of S-methyldithio  
617 carbazate, SMDTC (1.222 g, 0.01 mol) dissolved in hot ethanol (150 mL). The mixture was  
618 heated while being stirred to reduce the volume by half. The white precipitate formed from  
619 the mixture kept at 4°C overnight was filtered off, washed with cold ethanol and dried *in*  
620 *vacuo* over silica gel (yield 1.129 g, 70%). The compound was recrystallized from methanol  
621 and crystals suitable for X-ray diffraction analysis were obtained from the same solvent.  
622 Elemental analysis for  $\text{C}_{10}\text{H}_{18}\text{N}_4\text{S}_4$ : Calc. C 37.24, H 5.63, N 17.37; Found C 37.86, H 4.87,  
623 N 17.84.  $^1\text{H}$  NMR (300 MHz, DMSO- $d_6$ )  $\delta$  12.13 (s, 2H), 2.57 (s, 4H), 2.43 (s, 6H), 2.00 (s,  
624 6H).  $^{13}\text{C}$  NMR (75 MHz, DMSO- $d_6$ )  $\delta$  198.95, 157.63, 33.97, 17.77, 16.94. IR:  $\nu$  ( $\text{cm}^{-1}$ ) =  
625 3111 (m, b), 1628 (m), 1046 (s), 988 (m), 827 (m). UV-Vis in DMSO:  $\lambda_{\max}$  nm ( $\log \epsilon$  in  
626  $\text{L mol}^{-1} \text{cm}^{-1}$ ) = 276 (4.25), 305 (4.37),  $\approx 360$  (2.75, sh). RP-HPLC:  $R_T$  (min) = 6.4, 11.1, 18.7.  
627 Molar conductivity:  $\Lambda$  ( $\text{ohm}^{-1} \text{cm}^2 \text{mol}^{-1}$ ) = 3.58

628

### 629 5.2.3. Synthesis of CuSBHD

630 CuSBHD was prepared by adding copper(II) acetate monohydrate (0.020 g, 0.0001  
631 mol) in acetonitrile (20 mL) to a solution of SBHDH2 (0.047 g, 0.0001 mol) in acetonitrile  
632 (150 mL) at room temperature. The solution was stirred for an hour and then concentrated to  
633 reduce the volume before being placed at 4°C overnight. The product was filtered off and  
634 recrystallized from acetonitrile (yield 0.039 g, 73%). Black crystals of diffraction quality  
635 were crystallized from acetonitrile after several days through slow evaporation at 4°C.  
636 Elemental analysis for  $\text{C}_{22}\text{H}_{25}\text{CuN}_4\text{S}_4$ : Calc. C 49.27, H 4.51, N 11.85; Found C 49.40, H  
637 4.63, N 10.46. ESI-MS:  $m/z$  =  $[\text{M}+\text{H}]^+$  Calc. 536.04, Found 536.02;  $[\text{M}+\text{Na}]^+$  Calc. 558.02,  
638 Found 558.01;  $[\text{M}+\text{K}]^+$  Calc. 573.99, Found 573.98;  $[\text{2M}+\text{3H}]^+$  Calc. 1073.08, Found  
639 1073.04. IR:  $\nu$  ( $\text{cm}^{-1}$ ) = 1629 (m), 1606 (w), 992 (s), 955 (s), 857 (m). UV-Vis in DMSO:  $\lambda_{\max}$   
640 nm ( $\log \epsilon$  in  $\text{L mol}^{-1} \text{cm}^{-1}$ ) = 275 (4.37),  $\approx 294$  (4.26, sh),  $\approx 340$  (4.01, sh),  $\approx 400$  (3.55, sh),  
641  $\approx 600$  (2.45, sh). RP-HPLC:  $R_T$  (min) = 28.5. Magnetic moment:  $\mu$  (B.M.) = 1.48. Molar  
642 conductivity:  $\Lambda$  ( $\text{ohm}^{-1} \text{cm}^2 \text{mol}^{-1}$ ) = 13.01.

643

#### 644 5.2.4. Synthesis of CuSMHD

645 CuSMHD was prepared by adding copper(II) acetate monohydrate (0.200 g, 0.001  
646 mol) in methanol (20 mL) to a hot solution of SMHDH2 (0.322 g, 0.001 mol) in methanol  
647 (100 mL). The reaction was heated until the volume reduced to half and then placed at 4°C  
648 overnight. The product was filtered off and recrystallized from acetonitrile to afford 0.296 g  
649 of CuSMHD (yield 77%). Black crystals of diffraction quality crystallized from acetonitrile  
650 after several weeks through slow evaporation at room temperature. Elemental analysis for:  
651 C<sub>10</sub>H<sub>17</sub>CuN<sub>4</sub>S<sub>4</sub>: Calc. C 31.27, H 4.20, N 14.59; Found C 31.35, H 4.24, N 14.64. ESI-MS:  
652  $m/z = [M + H]^+$  Calc. 383.97, Found 383.96;  $[M+Na]^+$  Calc. 405.96, Found 405.94;  $[M+K]^+$   
653 Calc. 421.93, Found 421.92. IR:  $\nu$  (cm<sup>-1</sup>) = 1628 (m), 1611(w), 1000 (s), 964 (s), 821 (m).  
654 UV-Vis in DMSO:  $\lambda_{\max}$  nm (log  $\epsilon$  in L mol<sup>-1</sup> cm<sup>-1</sup>) = 273 (4.34),  $\approx$ 294 (4.24, sh),  $\approx$ 340 (3.99,  
655 sh),  $\approx$ 400 (3.49, sh)  $\approx$ 600 (2.43, sh). RP-HPLC: R<sub>T</sub> (min) = 23.3. Magnetic moment:  $\mu$  (B.M.)  
656 = 1.66. Molar conductivity:  $\Lambda$  (ohm<sup>-1</sup> cm<sup>2</sup> mol<sup>-1</sup>) = 12.80.

657

#### 658 5.2.5. Synthesis of SBPY

659 SBPY was a side product from the initial attempt to synthesize SBHDH2 using  
660 prolonged heating. Single crystals of diffraction quality were obtained from DMSO and  
661 analyzed by single crystal X-ray diffraction. ESI-MS:  $m/z = [M + H]^+$  Calc. 277.08, Found  
662 277.08;  $[M + Na]^+$  Calc. 299.07, Found 299.06. <sup>1</sup>H NMR (300 MHz, DMSO-d<sub>6</sub>):  $\delta$  (ppm) =  
663 12.29 (s, 1H), 7.45 – 7.20 (m, 5H), 5.69 (s, 2H), 4.45 (s, 2H), 2.00 (s, 6H). <sup>13</sup>C NMR (75  
664 MHz, DMSO-d<sub>6</sub>):  $\delta$  (ppm) = 204.09, 136.30, 129.02, 128.55, 127.43, 126.50, 104.34, 38.17,  
665 10.99. IR:  $\nu$  (cm<sup>-1</sup>) = 3264 (m), 2917 (w), 1055 (s), 972 (w), 828 (w). UV-Vis in DMSO:  $\lambda_{\max}$   
666 nm (log  $\epsilon$  in L mol<sup>-1</sup> cm<sup>-1</sup>) = 282 (4.02). RP-HPLC: R<sub>T</sub> (min) = 22.3.

667

### 668 5.3. Biological studies

#### 669 5.3.1. Antimicrobial assay

##### 670 5.3.1.1. Bacterial strains, culture media and chemicals

671 The bacteria used in this study are listed in Table 7. The microorganisms studied  
672 included reference (from the American Type Culture Collection) and clinical (Laboratory  
673 collection) strains of Gram-negative bacteria *Escherichia coli*, *Enterobacter aerogenes*,  
674 *Acinetobacter baumannii*, *Klebsiella pneumoniae*, *Pseudomonas aeruginosa* and *Salmonella*  
675 *enterica* serotype Typhimurium as well as Gram-positive strain *Staphylococcus aureus*.  
676 EA289 is an *E. aerogenes* KAN<sup>S</sup> (susceptible to kanamycin, MDR isolate that exhibits active

677 efflux of norfloxacin and AcrAB-TolC pump overproduction), EA294 and EA298 derived  
 678 from EA289 and deleted of AcrA and TolC, respectively [77]. AG100 is an *E. coli* Wild Type  
 679 (WT) and AG100A is its KAN<sup>R</sup> (resistant to kanamycin) derivative, deleted of AcrAB and  
 680 hypersensitive to chloramphenicol, tetracycline, ampicillin and nalidixic acid [78]. Strains  
 681 were grown at 37°C on Mueller-Hinton medium 24 h prior to any assay. Mueller-Hinton  
 682 broth (MHB) was used for the susceptibility test. Polymyxin B nonapeptide (PMBN) was  
 683 obtained from Sigma-Aldrich and the culture medium was purchased from Becton Dickinson.

684 Table 7: Bacterial strains.

Bacteria strains	Features	References
<b><i>Escherichia coli</i></b>		
AG100	Wild-type <i>E. coli</i> K-12	[78]
AG100A	AG100 $\Delta$ AcrAB::KAN <sup>R</sup>	[78]
<b><i>Enterobacter aerogenes</i></b>		
EA289	KAN sensitive derivative of EA27	[77]
EA294	EA289 AcrA::KAN <sup>R</sup>	[77]
EA298	EA 289 TolC::KAN <sup>R</sup>	[77]
<b><i>Acinetobacter baumannii</i></b>		
ATCC19606	Reference strain	-
<b><i>Klebsiella pneumoniae</i></b>		
ATCC12296	Reference strain	-
<b><i>Pseudomonas aeruginosa</i></b>		
PA 01	Reference strain	-
<b><i>Salmonella enterica</i> serotype Typhimurium</b>		
SL696	Wild-type, metA22, trpB2, strAi20	[79]
<b><i>Staphylococcus aureus</i></b>		
SA1199	Wild-type clinical, methicillin-susceptible	[80]

716 KAN<sup>R</sup>, resistance to kanamycin

717 5.3.1.2. *Determination of bacterial susceptibility*

718 The respective minimum inhibitory concentrations (MIC) of the samples against  
719 targeted bacteria were determined using the microdilution method (CLSI) [81].  
720 Susceptibilities were determined in 96-well microplates with an inoculum of  $2 \times 10^5$  cfu in  
721 200  $\mu$ L of MHB containing two-fold serial dilutions of samples. MICs were determined in  
722 the presence of 5% or 0.5% of DMSO. In the first case, a 20 $\times$  concentration range of each  
723 compound was prepared in DMSO 100%. In the second case, a 200 $\times$  concentration range of  
724 each compound was prepared in DMSO 100% and then diluted with H<sub>2</sub>O to obtain a 20 $\times$   
725 concentration range in DMSO 10%. 10  $\mu$ l was added to 190  $\mu$ l of inoculum reducing the  
726 DMSO concentration to 0.5%. The MICs of samples were determined after 18 h incubation at  
727 37°C, following addition (50  $\mu$ l) of 0.2 mg/mL iodonitrotetrazolium (INT) and incubation at  
728 37°C for 30 minutes. MIC is defined as the lowest sample concentration that prevented the  
729 color change of the medium and exhibited complete inhibition of microbial growth. The  
730 sample dilution range was from 0-128  $\mu$ M. Samples were tested alone or in the presence of  
731 PMBN at 1/5 of its direct MIC (51.2 mg/L or 102.4 mg/L final concentration). All assays  
732 were performed in duplicate or triplicate.

733

734 5.3.2. *In vitro cytotoxicity testing*

735 MCF-7 (human breast cancer cells possessing nuclear estrogen receptor) and MDA-  
736 MB-231 (human breast cancer cells without nuclear estrogen receptor) were obtained from  
737 the National Cancer Institute, U.S.A. Both cell lines were cultured in RPMI-1640 / DMEM  
738 (High glucose) (Sigma) medium supplemented with 10% fetal calf serum. The cells were  
739 plated into 96-well plates at a cell density of 6000 cells/well. After incubation for 24 hours,  
740 the medium was discarded and the cells were rinsed with PBS solution. 200  $\mu$ L of a series of  
741 concentrations (50.0, 25.0, 10.0, 5.0, 1.0 and 0.5  $\mu$ M) for each sample was added to each  
742 well. The plate was incubated for another 72 hours. Cytotoxicity was determined using the  
743 microtitration of 3-(4,5-dimethylthiazol-2-yl)-2,5-diphenyltetrazolium bromide (MTT) assay  
744 (Sigma, USA) as reported by Mosmann [75]. MTT solution (20 $\mu$ L, 5 mg/mL) was added to  
745 each well. The plate was wrapped with aluminium foil and incubated for 4 h after which the  
746 MTT solution was discarded leaving formazan crystals. 200  $\mu$ L of DMSO was added to each  
747 well to dissolve the formazan. The effect of the compound on cell line viability was measured  
748 on an automated spectrophotometric plate reader (model MRX II Elisa microplate reader) at a

749 test wavelength of 570 nm. Cytotoxicity was expressed as IC<sub>50</sub>, i.e. the concentration that  
750 reduced the absorbance of treated cells by 50% with reference to the control (untreated cells).  
751 IC<sub>50</sub> values were determined from the plotted absorbance data for the dose-response curves.  
752 Controls that contained only cells were included for each sample. Tamoxifen was used as the  
753 cytotoxic standard.

754

#### 755 5.4. X-ray crystallography

756 X-ray diffraction measurements for SBPY were performed at 100 K on a Bruker  
757 Kappa X8 APEXII CD diffractometer with graphite monochromatised MoK $\alpha$  radiation ( $\lambda =$   
758  $0.71073 \text{ \AA}$ ). Correction for absorption was based on a multi-scan technique [82]. Intensity  
759 data for SMHDH2, CuSMHD and CuSBHD were measured at 150 K on an Oxford  
760 Diffraction Gemini CCD diffractometer employing either CuK $\alpha$  (SMHDH2),  $\lambda = 1.54184 \text{ \AA}$ ,  
761 or MoK $\alpha$  radiation (CuSMHD and CuSBHD). Corrections for absorption were based on a  
762 multi-scan technique [83]. The structures were solved by direct methods and refined using  
763 anisotropic displacement parameters, H atoms in the riding model approximation and a  
764 weighting scheme of the form  $w = 1/[\sigma^2(F_o^2) + aP^2 + bP]$  where  $P = (F_o^2 + 2F_c^2)/3$  using  
765 SHELX programs [84] through the WinGX interface [85]. Crystal data and refinement details  
766 are collected in Table 1. The molecular structures shown in Figs 1-4 were drawn with 70%  
767 displacement ellipsoids using ORTEP-3 for Windows [85]. The overlay diagram, Fig. 4b, was  
768 drawn with QMol [86] and the crystal packing diagrams with DIAMOND [87].

769

#### 770 Acknowledgements

771 Support for the project came from Universiti Putra Malaysia (UPM), the Ministry of Higher  
772 Education (Malaysia), French ANR Blanc 2010, METABACT grant and the French  
773 Infrastructure for Integrated Structural Biology (FRISBI) ANR-10-INSB-05-01. M. L. Low is  
774 grateful for the award of an Erasmus Mundus: Maheva Scholarship and a UPM Graduate  
775 Research Fellowship (GRF).

776

777

778 **List of abbreviations**

779

<i>A. baumannii</i>	<i>Acinetobacter baumannii</i>
CV	Cyclic voltammetry
DMEM	Dulbecco's modified Eagle's medium
DMF	Dimethylformamide
DMSO	Dimethyl sulfoxide
DMSO-d6	Deuterated dimethyl sulfoxide
<i>E. aerogenes</i>	<i>Enterobacter aerogenes</i>
<i>E. coli</i>	<i>Escherichia coli</i>
EPR	Electron paramagnetic resonance
ESI-MS	Electrospray ionization-mass spectrometry
FT-IR	Fourier transform-infrared spectroscopy
INT	Iodonitrotetrazolium
KAN <sup>R</sup>	Resistance to kanamycin
KAN <sup>S</sup>	Sensitive to kanamycin
<i>K. pneumonia</i>	<i>Klebsiella pneumonia</i>
LMCT	Ligand-to-metal charge transfer
MCF-7	Human breast carcinoma cells expressing nuclear estrogen receptors
MDA-MB-231	Human breast carcinoma cells not expressing nuclear estrogen receptors
MDR	Multidrug resistance
MHB	Mueller-Hinton broth
MIC	Minimum inhibitory concentration
MTT	3-(4,5-dimethylthiazol-2-yl)-2,5-diphenyltetrazolium bromide
NMR	Nuclear magnetic resonance
ORTEP	Oak Ridge thermal ellipsoid plot
PBS	Phosphate buffered saline
PMBN	Polymyxin B nonapeptide
<i>P. aeruginosa</i>	<i>Pseudomonas aeruginosa</i>
ROS	Reactive oxygen species
RP-HPLC	Reversed phase-high performance liquid chromatography
r. t.	Room temperature
<i>S. enterica</i>	<i>Salmonella enterica</i>
SBDTC	S-benzylidithiocarbazate
SMDTC	S-methyldithiocarbazate
SOD	Superoxide dismutase
<i>S. aureus</i>	<i>Staphylococcus aureus</i>
UV-Vis	Ultraviolet-visible
WT	Wild type

780

781

782 **Appendix A. Supplementary data**

783 Supplementary data related to this article can be found at .....

784 Crystallographic data for the structures reported herein have been deposited with the  
785 Cambridge Crystallographic Data Centre, CCDC No. 1057065 for SBPY, 1057066 for  
786 SMHDH2, 1057067 for CuSMHD and 1057068 for CuSBHD. Copies of this information  
787 may be obtained from the Director, CCDC, 12 Union Road, Cambridge CB2 1EZ, UK (fax:  
788 +44-1223-336033; E-mail: [deposit@ccdc.cam.ac.uk](mailto:deposit@ccdc.cam.ac.uk) or <http://www.ccdc.cam.ac.uk>).

789

790 **References:**

791 [1] A. Coates, Y. Hu, R. Bax, C. Page, *Nat. Rev. Drug Discov.* 1 (2002) 895-910.

792 [2] G. Taubes, *Science* 321 (2008) 321, 356-361.

793 [3] J.-M. Pagès, L. Amaral, *Biochim. Biophys. Acta - Proteins Proteom.* 1794 (2009) 826-  
794 833.

795 [4] H. Nikaido, J.-M. Pagès, *FEMS Microbiol. Rev.* 36 (2012) 340-363.

796 [5] J. Ma, A. Jemal, in *Breast Cancer Metastasis and Drug Resistance*, Springer New York  
797 (2013) pp. 1-18.

798 [6] G. Yang, S. Nowsheen, K. Aziz, A. G. Georgakilas, *Pharmacol. Ther.* 139 (2013) 392-404.

799 [7] M. A. Ali, A. H. Mirza, R. J. Butcher, M. T. H. Tarafder, T. B. Keat, A. M. Ali, *J. Inorg.*  
800 *Biochem.* 92 (2002) 141-148.

801 [8] A. B. Beshir, S. K. Guchhait, J. A. Gascón, G. Fenteany, *Bioorg. Med. Chem. Lett.* 18  
802 (2008) 498-504.

803 [9] M. L. Low, L. Maigre, P. Dorlet, R. Guillot, J.-M. Pagès, K. A. Crouse, C. Policar, N.  
804 Delsuc, *Bioconjugate Chem.* 25 (2014) 2269-2284.

805 [10] M. R. Maurya, S. Khurana, A. Azam, W. Zhang, D. Rehder, *Eur. J. Inorg. Chem.* 2003  
806 (2003) 1966-1973.

807 [11] P. I. D. S. Maia, A. G. D. A. Fernandes, J. J. N. Silva, A. D. Andricopulo, S. S. Lemos, E.  
808 S. Lang, U. Abram, V. M. Deflon, *J. Inorg. Biochem.* 104 (2010) 1276-1282.

809 [12] F. R. Pavan, P. I. D. S. Maia, S. R. A. Leite, V. M. Deflon, A. A. Batista, D. N. Sato, S. G.  
810 Franzblau, C. Q. F. Leite, *Eur. J. Med. Chem.* 45 (2010) 1898-1905.

811 [13] T. B. S. A. Ravoof, K. A. Crouse, M. I. M. Tahir, F. N. F. How, R. Rosli, D. J. Watkins,  
812 *Transit. Metal Chem.* 35 (2010) 871-876.

813 [14] F. N. F. How, K. A. Crouse, M. I. M. Tahir, M. T. H. Tarafder, A. R. Cowley, *Polyhedron*  
814 27 (2008) 3325-3329.

- 815 [15] M. A. F. A. Manan, M. I. M. Tahir, K. A. Crouse, R. Rosli, F. N. F. How, D. J. Watkin, J.  
816 Chem. Crystallogr. 41 (2011) 1866-1871.
- 817 [16] J. P. Jasinski, J. R. Bianchani, J. Cueva, F. A. El-Saied, A. A. El-Asmy, D. X. West, Z.  
818 Anorg. Allg. Chem. 629 (2003) 202-206.
- 819 [17] M. A. Ali, S. E. Livingstone, Coord. Chem. Rev. 13 (1974) 101-132.
- 820 [18] M. T. H. Tarafder, A. M. Ali, Y. W. Wong, S. H. Wong, K. A. Crouse, Synth. React.  
821 Inorg. Met.-Org. Chem. 31 (2001) 115-125.
- 822 [19] M. L. Low, G. Paulus, P. Dorlet, R. Guillot, R. Rosli, N. Delsuc, K. A. Crouse, C.  
823 Policar, Biometals, 28 (2015) 553-566
- 824 [20] P.A. Vigato, S. Tamburini, Coord. Chem. Rev. 248 (2004) 1717-2128.
- 825 [21] J. P. Holland, P. J. Barnard, S. R. Bayly, H. M. Betts, G. C. Churchill, J. R. Dilworth, R.  
826 Edge, J. C. Green, R. Hueting, Eur. J. Inorg. Chem. 2008 (2008) 1985-1993.
- 827 [22] M. Gennari, J. Pécaut, M. N. Collomb, C. Duboc, Dalton Trans. 41 (2012) 3130-3133.
- 828 [23] B. M. Paterson, P. S. Donnelly, Chem. Soc. Rev. 40 (2011)3005-3018; P. S. Donnelly,  
829 Dalton Trans. 40 (2011) 999-1010.
- 830 [24] A. Díaz, R. Pogni, R. Cao, R. Basosi, Inorg. Chim. Acta 275-276 (1998) 552-556.
- 831 [25] A. Díaz, R. Cao, A. Fragosó, I. Sánchez, Inorg. Chem. Commun. 2 (1999) 361-363.
- 832 [26] K. Y. Djoko, M.M. Goytia, P. S. Donnelly, M. A. Schembri, W. M. Shafer, A. G.  
833 McEwan, *Antimicrob. Agents Chemother.* 59 (2015), 6444-6453.
- 834 [27] Q.-X. Li, H.-A. Tang, Y.-Z. Li, M. Wang, L.-F. Wang, C.-G. Xia, J. Inorg. Biochem. 78  
835 (2000) 167-174.
- 836 [28] Z. Afrasiabi, E. Sinn, S. Padhye, S. Dutta, S. Padhye, C. Newton, C. E. Anson, A. K.  
837 Powell, J. Inorg. Biochem. 95 (2003) 306-314.
- 838 [29] T. Ngarivhume, A. Díaz, R. Cao, M. Ortiz, I. Sánchez, Synth. React. Inorg. Met.-Org.  
839 Nano-Met Chem 35 (2005) 795-800.
- 840 [30] M. A. Ali, C. M. Haroon, M. Nazimuddin, S. M. M. U. H. Majumder, M. T. H. Tarafder,  
841 M. A. Khair, Transit. Metal Chem. 17 (1992) 133-136.
- 842 [31] X. H. Zhu, S. H. Liu, Y. J. Liu, J. Ma, C. Y. Duan, X. Z. You, Y. P. Tian, F. X. Xie, S. S.  
843 Ni, Polyhedron 18 (1998) 181-185.
- 844 [32] M. A. Ali, P. V. Bernhardt, M. A. H. Brax, J. England, A. J. Farlow, G. R. Hanson, L. L.  
845 Yeng, A. H. Mirza, K. Wieghardt, Inorg. Chem. 52 (2013) 1650-1657.
- 846 [33] M. H. E. Chan, K. A. Crouse, M. I. M. Tahir, R. Rosli, N. Umar-Tsafe, A. R. Cowley,  
847 Polyhedron 17 (2008) 1141-1149.

- 848 [34] K. B. Chew, M. T. H. Tarafder, K. A. Crouse, A. M. Ali, B. M. Yamin, H. K. Fun,  
849 Polyhedron 23 (2004) 1385-1392.
- 850 [35] M. A. Ali, S. M. G. Hossain, S. M. M. H. Majumder, M. N. Uddin, M. T. H. Tarafder,  
851 Polyhedron 6 (1987) 1653-1656.
- 852 [36] R. N. Patel, K. K. Shukla, A. Singh, M. Choudhary, D. K. Patel, J. Niclós-Gutiérrez, D.  
853 Choquesillo-Lazarte, *Transit. Metal Chem.* 34 (2009) 239-245.
- 854 [37] A. T. Chaviara, P. J. Cox, K. H. Repana, A. A. Pantazaki, K. T. Papazisis, A. H.  
855 Kortsaris, D. A. Kyriakidis, G. S. Nikolov, C. A. Bolos, *J. Inorg. Biochem.* 99 (2005)  
856 467-476.
- 857 [38] B. Jeragh, A. A. El-Asmy, *Spectrochim. Acta A: Mol. Biomol. Spectrosc.* 130 (2014)  
858 546-552.
- 859 [39] B. Jeragh, A. A. El-Asmy, *Spectrochim. Acta A: Mol. Biomol. Spectrosc.* 129 (2014)  
860 307-313.
- 861 [40] K. Liu, H. Lu, L. Hou, Z. Qi, C. Teixeira, F. Barbault, B. T. Fan, S. Liu, S. Jiang, L. Xie,  
862 *J. Med. Chem.* 51 (2008) 7843-7854.
- 863 [41] A. Fürstner, *Angew. Chem. Int. Ed.* 42 (2003) 3582-3603.
- 864 [42] P. F. Rapheal, E. Manoj, M. R. Prathapachandra Kurup, *Polyhedron* 26 (2007) 818-828.
- 865 [43] K. A. Crouse, K.-B. Chew, M. T. H. Tarafder, A. Kasbollah, A. M. Ali, B. M. Yamin, H.  
866 K. Fun, *Polyhedron* 23 (2004) 161-168.
- 867 [44] M. A. Ali, M. T. H. Tarafdar, *J. Inorg. Nucl. Chem.* 39 (1977) 1785-1791.
- 868 [45] S. Belaid, A. Landreau, S. Djebbar, O. Benali-Baitich, G. Bouet, J.-P. Bouchara, *J. Inorg.*  
869 *Biochem.* 102 (2008) 63-69.
- 870 [46] M. Kato, H. B. Jonassen, J. C. Fanning, *Chem. Rev.* 64 (1964) 99-128.
- 871 [47] M. S. Nair, R.S. Joseyphus, *Spectrochim. Acta A: Mol. Biomol. Spectrosc.* 70 (2008)  
872 749-753.
- 873 [48] V. P. Singh, D.P. Singh, *Macromol. Res.* 21 (2013) 757-766.
- 874 [49] A. K. Nandi, S. Chaudhuri, S. K. Mazumdar, S. Ghosh, *Inorg. Chim. Acta* 92 (1984)  
875 235-240.
- 876 [50] P. J. Blower, T. C. Castle, A. R. Cowley, J. R. Dilworth, P. S. Donnelly, E. Labisbal, F. E.  
877 Sowrey, S. J. Teat, M. J. Went, *Dalton Trans.* (2003) 4416-4425.
- 878 [51] A. R. Cowley, J. R. Dilworth, P. S. Donnelly, A. D. Gee, J. M. Heslop, *Dalton Trans.*  
879 (2004) 2404-2412.
- 880 [52] B. M. Paterson, J. A. Karas, D. B. Scanlon, J. M. White, P. S. Donnelly, *Inorg. Chem.* 49  
881 (2010) 1884-1893.

- 882 [53] M. A. Ali, A. H. Mirza, R. J. Fereday, R. J. Butcher, J. M. Fuller, S. C. Drew, L. R.  
883 Gahan, G. R. Hanson, B. Moubaraki, K. S. Murray, *Inorg. Chim. Acta* 358 (2005) 3937-  
884 3948.
- 885 [54] M. T. H. Tarafder, M. Ali, D. J. Wee, K. Azahari, S. Silong, K. A. Crouse, *Transit. Metal*  
886 *Chem.* 25 (2000) 456-460.
- 887 [55] R. Hueting, M. Christlieb, J. R. Dilworth, E. G. Garayoa, V. Gouverneur, M. W. Jones, V.  
888 Maes, R. Schibli, X. Sun, D. A. Tourwe, *Dalton Trans.* 39 (2010) 3620-3632.
- 889 [56] R. C. Chikate, A. R. Belapure, S. B. Padhye, D. X. West, *Polyhedron* 24 (2005) 889-899.
- 890 [57] D. Kivelson, R. Neiman, *J. Chem. Phys.* 35 (1961) 149-155.
- 891 [58] S. Chandra, X. Sangeetika, *Spectrochim. Acta A: Mol. Biomol. Spectrosc.* 60 (2004)  
892 147-157.
- 893 [59] P. Murali Krishna, K. Hussain Reddy, J. Pandey, D. Siddavattam, *Transit. Metal Chem.*  
894 33 (2008) 661-668.
- 895 [60] J. Joseph, K. Nagashri, G. B. Janaki, *Eur. J. Med. Chem.* 49 (2012) 151-163.
- 896 [61] Z. Duracková, M. A. Mendiola, M. T. Sevilla, A. Valent, *Bioelectrochem. Bioenerg.* 48  
897 (1999) 109-116.
- 898 [62] P. J. Jansson, P. C. Sharpe, P. V. Bernhardt, D. R. Richardson, *J. Med. Chem.* 53 (2012)  
899 5759-5769.
- 900 [63] M. T. Basha, J. D. Chartres, N. Pantarat, M. Akbar Ali, A. H. Mirza, D. S. Kalinowski,  
901 D. R. Richardson, P. V. Bernhardt, *Dalton Trans.* 41 (2012) 6536-6548.
- 902 [64] N. S. Ng, P. Leverett, D. E. Hibbs, Q. Yang, J. C. Bulanadi, M. Jie Wu, J. R. Aldrich-  
903 Wright, *Dalton Trans.* 42 (2012) 3196-3209.
- 904 [65] R. Notman, M. Noro, B. O'Malley, J. Anwar, *J. Am. Chem. Soc.* 128 (2006) 13982-  
905 13983.
- 906 [66] Z.-W. Yu, P. J. Quinn, *Mol. Membr. Biol.* 15 (1998) 59-68.
- 907 [67] C. N. Dolan, R. D. Moriarty, E. Lestini, M. Devocelle, R. J. Forster, T. E. Keyes, J.  
908 *Inorg. Biochem.* 119 (2012) 65-74.
- 909 [68] M. A. Randhawa, *Jpn. J. Med. Mycol.* 47 (2006) 314-318.
- 910 [69] B.M. Ghajar, S. A. Harmon, *Biochem. Biophys. Res. Commun.* 32 (1968) 940-944.
- 911 [70] H. C. Ansel, W. P. Norred, I. L. Roth, *J. Pharm. Sci.* 58 (1969) 836-839.
- 912 [71] E. Goemaere, A. Melet, V. R. Larue, A. I. Lieutaud, R. A. De Sousa, J. Chevalier, L.  
913 Yimga-Djapa, C. Giglione, F. Huguet, M. Alimi, *J. Antimicrob. Chemother.* 67 (2012)  
914 1392-1400.

- 915 [72] M. E. Hossain, M. N. Alam, J. Begum, M. Akbar Ali, M. Nazimuddin, F. E. Smith, R. C.  
916 Hynes, *Inorg. Chim. Acta* 249 (1996) 207-213.
- 917 [73] J. A. Lessa, D. C. Reis, J. G. Da Silva, L. T. Paradizzi, N. F. Da Silva, M. De Fátima A.  
918 Carvalho, S. A. Siqueira, H. Beraldo, *Chem. Biodivers.* 9 (2012) 1955-1966.
- 919 [74] J. M. Bolla, S. Alibert-Franco, J. Handzlik, J. Chevalier, A. Mahamoud, G. Boyer G, K.  
920 Kiec-Kononowicz, J.-M. Pagès, *FEBS Lett.* 585 (2011) 1682-1690.
- 921 [75] T. Mosmann, *J. Immunol. Methods* 65 (1983) 55-63.
- 922 [76] Z. Afrasiabi, E. Sinn, S. Padhye, S. Dutta, S. Padhye, C. Newton, C. E. Anson, A. K.  
923 Powell, *J. Inorg. Biochem.* 95 (2003) 306-314.
- 924 [77] E. Pradel, J.-M. Pages, *Antimicrob. Agents Chemother.* 46 (2002) 2640-2643.
- 925 [78] M. Viveiros, A. Jesus, M. Brito, C. Leandro, M. Martins, D. Ordway, A. M. Molnar, J.  
926 Molnar, L. Amaral, *Antimicrob. Agents Chemother.* 49 (2005) 3578-3582.
- 927 [79] P. Plesiat, H. Nikaido, *Mol. Microbiol.* 6 (1992) 1323-1333.
- 928 [80] G. W. Kaatz, S. L. Barriere, D. R. Schaberg, R. Fekety, *J. Antimicrob. Chemother.* 20  
929 (1987) 753-758.
- 930 [81] V. Kuete, S. Alibert-Franco, K. Eyong, B. Ngameni, G. Folefoc, J. Nguemeving, J.  
931 Tangmouo, G. Fotso, J. Komguem, B. Ouahouo, *Int. J. Antimicrob. Agents* 37 (2011)  
932 156-161.
- 933 [82] G.M. Sheldrick, SADABS. University of Göttingen, Germany (1996).
- 934 [83] CrysAlis PRO, Agilent Technologies, Yarnton, Oxfordshire, England (2011).
- 935 [84] G.M. Sheldrick, *Acta Crystallogr. Sect. C*, 71 (2015) 3-8.
- 936 [85] L. J. Farrugia, *J. Appl. Crystallogr.* 32 (1999) 837-838.
- 937 [86] J. Gans, D. Shalloway, *J. Molec. Graphics Model.* 19 (2001) 557-559.
- 938 [87] K. Brandenburg, DIAMOND. Crystal Impact GbR, Bonn, Germany (2006).
- 939

**Highlights**

- Cu(II) complexes of dithiocarbazato 2,5-hexanedione Schiff bases were synthesized.
- Structures of four compounds were determined by single crystal X-ray diffraction.
- Compounds were active toward 10 Gram-positive and Gram-negative bacterial strains.
- Effects of efflux pumps and membrane penetration on activity are reported.
- Cu complexes are strongly active against MDA-MB-231 and MCF-7 cancer cell lines.